

See discussions, stats, and author profiles for this publication at: <https://www.researchgate.net/publication/260104921>

Oxidation State Imaging of Ceria Island Growth on Re(0001)

ARTICLE *in* THE JOURNAL OF PHYSICAL CHEMISTRY C · JULY 2013

Impact Factor: 4.77 · DOI: 10.1021/jp405887h

CITATIONS

8

READS

63

7 AUTHORS, INCLUDING:



[David Grinter](#)

Brookhaven National Laboratory

15 PUBLICATIONS 101 CITATIONS

[SEE PROFILE](#)



[Bruno Santos](#)

Ford Motor Company

167 PUBLICATIONS 1,652 CITATIONS

[SEE PROFILE](#)



[Tevfik Onur Menteş](#)

Sincrotrone Trieste S.C.p.A.

129 PUBLICATIONS 1,153 CITATIONS

[SEE PROFILE](#)



[Andrea Locatelli](#)

Sincrotrone Trieste S.C.p.A.

196 PUBLICATIONS 2,412 CITATIONS

[SEE PROFILE](#)

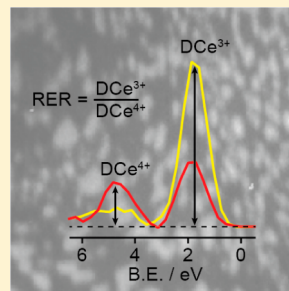
Oxidation State Imaging of Ceria Island Growth on Re(0001)

David C. Grinter,[†] Chi-Ming Yim,[†] Chi L. Pang,[†] Benito Santos,[‡] Tevfik O. Mentes,[‡] Andrea Locatelli,[‡] and Geoff Thornton^{*,†}

[†]Department of Chemistry and London Centre for Nanotechnology, University College London, 20 Gordon Street, London WC1H 0AJ, United Kingdom

[‡]Elettra - Sincrotrone Trieste S.C.p.A., S.S. 14, km 163.5 in Area Science Park, 34149 Basovizza, Trieste, Italy

ABSTRACT: High resolution X-ray photoemission electron microscopy (XPEEM) and low energy electron microscopy (LEEM) have been used to investigate the growth of ultrathin CeO_x(111) on Re(0001), a model catalyst system. Rotational domains of CeO_x(111) are identified with microprobe low energy electron diffraction (LEED) and dark-field LEEM. In the regions not covered by the ceria islands, a surface rhenium-oxide layer has been observed using energy-filtered XPEEM imaging and spectroscopy. The oxidation state of the ceria is key to its catalytic activity. For this reason we have employed resonant photoelectron spectroscopy of the Ce 4f contributions to the valence band to monitor the relative Ce³⁺ and Ce⁴⁺ concentrations. The overall stoichiometry of the moderately reduced film was CeO_{1.63}. Resonant energy-filtered XPEEM imaging of the Ce oxidation state allowed us to confirm the uniformity of this stoichiometry across the ceria islands that constituted the film.



INTRODUCTION

As model systems for the study of heterogeneous catalysis, ultrathin metal oxide films have been of significant interest over the past decade. Ceria (CeO₂) has been particularly in vogue due to its numerous industrial applications in a variety of fields, notably in connection with catalysis of the low temperature water-gas-shift reaction in combination with gold nanoparticles.^{1–3} Preparing ceria films of a few nanometre thickness on conducting substrates, such as Pt(111),⁴ Ru(0001),⁵ Rh(111),⁶ and Cu(111),⁷ permits the application of the full arsenal of electron-based surface science techniques to study their structure and reactivity.

Synchrotron-based X-ray photoemission electron microscopy (XPEEM) has previously been used to investigate ultrathin metal oxides.⁸ XPEEM and high resolution low energy electron microscopy (LEEM) are powerful tools which have been used with effect in the analysis of ultrathin oxide film systems such as TiO_x/Pt(111)⁹ and VO_x/Rh(111)¹⁰ and recently ceria on Ru(0001)⁵ and Cu(111).⁷

Monitoring the oxidation state of cerium within ultrathin ceria films is typically performed in two different ways: (i) deconvolution of Ce 3d or 4d X-ray photoemission (XPS) core level spectra into Ce³⁺ and Ce⁴⁺ contributions⁶ and (ii) resonant photoemission of the Ce 4f level.¹¹ This resonant photoemission technique has been shown to be extremely sensitive to small changes in the Ce oxidation state and has been used to great effect in the study of ceria film reduction by deposition of various metals.¹² Here we describe an investigation of ultrathin ceria film growth on Re(0001), examining the morphology with LEEM and the stoichiometry of the oxide islands using resonant energy-filtered XPEEM.

EXPERIMENTAL PROCEDURE

The measurements were carried out at the Nanospectroscopy beamline (1.2L) at Elettra (Trieste, Italy) using the Elmitec spectroscopic photoemission and low-energy electron microscope (SPELEEM III). The SPELEEM combines LEEM and energy-filtered XPEEM into a single instrument, which uses electrons or soft X-rays as a probe to implement a variety of methods enabling structural or chemical sensitivity.¹³ The SPELEEM microscope can be operated in imaging mode (XPEEM and LEEM with 30 and 10 nm spatial resolution, respectively), diffraction mode (microprobe-ARPES and microprobe-LEED), and spectroscopy mode (microprobe-XPS). In XPEEM mode, the SPELEEM has an energy resolution better than 300 meV.¹⁴ In our experiments, we used LEEM in both the bright and dark field modes, respectively, employing primary or secondary diffracted beams for imaging.

The Re(0001) single crystal was prepared by repeated cycles of annealing to 1000 K in 1×10^{-6} mbar O₂ followed by flashing up to 2000 K in UHV until no contamination was observed in XPS and a well-ordered surface was observed in LEED and LEEM. A CeO_{2-x}(111) film was prepared by depositing ~0.8 MLE Ce metal (99.9%, Alfa-Aesar) in situ at room temperature from an electron-beam evaporator (Focus EFM-3) at a deposition rate of 0.05 ML min⁻¹. This was followed by annealing to 850 K in 1×10^{-7} mbar O₂ while monitoring the LEED until sharp ceria diffraction spots were observed (approximately 10 min). The evaporation rate of cerium was calibrated by monitoring the LEED pattern during

Received: June 14, 2013

Revised: July 16, 2013

Published: July 23, 2013



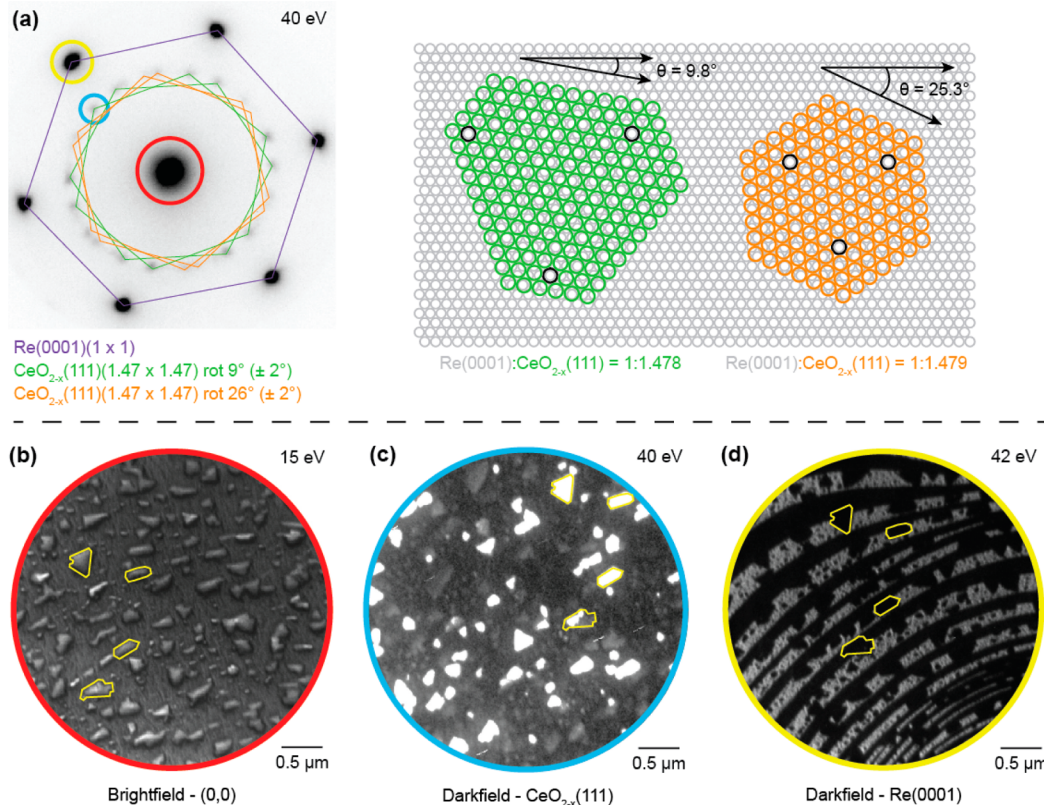


Figure 1. Low energy electron diffraction (LEED) and Microscopy (LEEM) images of a 0.8 MLE $\text{CeO}_{2-x}(111)$ ultrathin film on $\text{Re}(0001)$. (a) LEED ($E = 40$ eV) displaying the first-order (1×1) reflexes of the $\text{Re}(0001)$ substrate (purple highlight) as well as a ring of spots that originate from rotated domains of the ceria film at $\pm 9^\circ$ and $\pm 26^\circ$ (green and orange highlights respectively) with respect to the substrate. Corresponding models displaying the coincidences between the substrate and ceria lattices at these rotations are also shown. (b) Bright-field ($0,0$) LEEM ($E = 15$ eV, FOV = 4 μm) showing dispersed, well-defined islands of ceria displaying a mixture of triangular and pseudohexagonal shapes with lateral dimensions up to ~ 300 nm. (c) Dark-field LEEM ($E = 40$ eV, FOV = 4 μm) from one of the $\text{CeO}_{2-x}(111)$ diffraction spots (blue circle); the ceria islands with the corresponding LEED appear bright. (d) Dark-field LEEM ($E = 42$ eV, FOV = 4 μm) from one of the $\text{Re}(0001)$ diffraction spots (yellow circle); the alternating bright and dark stripes are the terraces of the $\text{Re}(0001)$ resulting from the underlying hcp symmetry, and the dark patches within the terraces correspond to ceria islands. The positions of four ceria islands have been marked in each of the LEEM images (b–d) and illustrate the thermal drift during measurement.

deposition according to the known epitaxial growth exhibited on $\text{W}(110)$.¹⁵ Ceria coverage is given in MLE where one monolayer is defined as the complete coverage of the surface by a single CeO_2 trilayer unit.

Image and spectral analysis were carried out using Igor Pro 6.22 (Wavemetrics), and photoemission spectra were fitted using Casa XPS vers. 2.3. Photon energies employed to record core level spectra were as follows: O 1s, 650 eV; Re 4f, 200 eV. For resonant spectra of Ce 4f, the photon energies used were 115, 120.5, and 123.5 eV corresponding to off-resonance, on-resonance Ce^{3+} , and on-resonance Ce^{4+} , respectively.¹¹ Binding energies for all spectra have been referenced to the Fermi level of the $\text{Re}(0001)$ substrate. Earlier LEEM and XPEEM measurements of ultrathin $\text{CeO}_{2-x}(111)$ films on $\text{Pt}(111)$ demonstrated that irradiation by either electrons ($E > 40$ eV) or the X-ray beam induced a disordered reduced structure of the top trilayer of ceria.¹⁶ We found out that measuring in a background pressure of 1×10^{-7} mbar O_2 prevents this damage; all of the images and spectra in this study were therefore obtained under the oxygen partial pressure. We note from our STM investigations that exposure of ceria ultrathin films to O_2 at room temperature does not modify the stoichiometry of the selvedge.

RESULTS AND DISCUSSION

One of the main strengths of the SPELEEM instrument is its ability to study dynamical processes in situ, such as monitoring ultrathin film growth. The LEED mode was initially employed. After Ce deposition the sample temperature was increased over a period of ~ 10 min in 1.1×10^{-7} mbar of O_2 until a ceria diffraction pattern was obtained at 850 K. The LEED pattern of a 0.8 MLE $\text{CeO}_{2-x}(111)$ film on $\text{Re}(0001)$ is presented in Figure 1a with the main features highlighted. The intense primary reflections from the Re substrate (purple highlight) form a (1×1) pattern with an inner ring of spots originating from the $\text{CeO}_{2-x}(111)$ film (green and orange highlights). The ceria spots are rotated with respect to the substrate by $\pm 9^\circ$ and $\pm 26^\circ$ (error in both is $\pm 2^\circ$) and presumably originate from rotated domains. Rotational domains are relatively common on such films and have previously been reported for $\text{CeO}_{2-x}(111)/\text{Ru}(0001)$ ⁵ and observed in our own STM investigations of $\text{CeO}_{2-x}(111)/\text{Pt}(111)$.¹⁷ The ratio of lattice constants between the $\text{CeO}_{2-x}(111)$ and the $\text{Re}(0001)$ derived from this LEED pattern is measured to be 1.47:1 and differs from the expected ratio of bulk lattice constants (1.39:1), suggesting that the ceria expands by $\sim 6\%$ relative to the bulk lattice. Similar observations have been made for other low-coverage ceria films where there is strain-induced contraction or expansion of

the oxide lattice due to the large mismatch with the metal supports.^{4,18,19} Also displayed in Figure 1a are models of the ceria and substrate lattices demonstrating the coincidence points after rotations of 9.8° (green) and 25.3° (orange) and a slight further expansion of the ceria lattice constant, but still well within the error estimates for our measurements.

A bright-field (BF) LEEM image of the film (using the specularly reflected electrons, highlighted with a red circle in Figure 1a) is shown in Figure 1b with a field of view (FOV) of 4 μm. The ceria forms isolated islands dispersed across the Re(0001) substrate with lateral dimensions ranging from 20 to 300 nm. The shapes and sizes of these islands are consistent with STM investigations of similar coverage films on Pt(111) and other noble metal surfaces.^{4,11,20} Dark-field (DF) LEEM imaging was also carried out using the diffracted beams for one of the ceria spots (blue) and one of the Re spots (yellow) in Figure 1a, as shown in Figure 1, panels c and d, respectively. These images were taken from the same region of the surface over a time period of a few minutes; by mapping the island positions, a drift of ~2 μm is observed over the course of acquisition as the sample cooled after oxidation. In the ceria DF image shown in Figure 1c (blue) the islands appear bright on a dark background. Different levels of brightness are observed for the islands. If the opposite rotated diffraction spot is used for illumination (not shown) then the contrast is inverted (dark islands become bright and vice versa). There are a variety of orientations of the edges of the ceria islands as expected from the lack of epitaxy between the ceria and the substrate and the many rotational domains evidenced by LEED. The contrast in the Re(0001) DF image displayed in Figure 1d (yellow) is dominated by alternating bright and dark stripes from the substrate terraces, which have widths of up to 200 nm, with the ceria islands forming dark shadows. The shapes and sizes of these shadows map perfectly with the bright islands in (Figure 1c) and the features in (Figure 1b), confirming their assignment as ceria. To act as a visual aid for this mapping, four ceria islands have been highlighted in each of the LEEM images (Figure 1b–d).

XPEEM imaging in the energy-filtered mode was used to provide spatially resolved XPS of the Re 4f region. A representative XPEEM image (FOV = 4 μm) obtained at a binding energy of 40.25 eV, which corresponds to the maximum of the Re 4f_{7/2} peak, is displayed in Figure 2. From this image we can identify the ceria islands which appear as dark patches on the surface with shapes and sizes consistent with the earlier LEEM images. By sampling regions within these islands (far from their edges) and also in between them, we can obtain XPS spectra exclusively from the Re(0001) substrate (blue curve) and from the CeO_{2-x}(111) film (black curve) as shown in Figure 2. Both spectra display the Re 4f doublet with Re 4f_{5/2} at 42.6 eV B.E. and Re 4f_{7/2} at 40.25 eV B.E., along with an additional doublet shifted by 1 eV to higher binding energy which is characteristic of a surface Re–O phase.²¹ In Ce XPEEM core level data shown below we demonstrate that there is no Ce present between the ceria islands.

A model of the ceria film is presented in Figure 3a, showing the CeO_{2-x}(111) islands as well as the Re–O layer in between them. The attenuation of the Re 4f signal by the ceria islands is clearly visible in Figure 2: Assuming an inelastic mean free path of 0.9 nm for 160 eV electrons in CeO₂,²² the island thickness is estimated at ~0.8 nm, or between 2 and 3 CeO₂ trilayers. The high-resolution LEEM image in Figure 3b permits an accurate measure of the fractional ceria area coverage over the

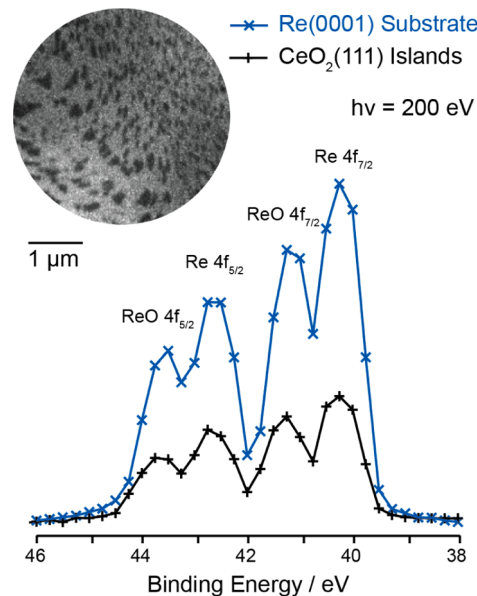


Figure 2. X-ray photoelectron spectroscopy (XPS) and X-ray photoemission electron microscopy (XPEEM) of the Re 4f region of a 0.8 MLE CeO_{2-x}(111) ultrathin film on Re(0001). In the inset energy-filtered XPEEM image (corresponding to a binding energy of 40.25 eV), the ceria islands appear as dark patches. The spectra were obtained by sampling regions in the center of these ceria islands (black curve) and from areas in between the islands (blue curve). In addition to the Re 4f spin–orbit doublet, a second doublet originating from a surface Re–O phase is also observed with a 1 eV shift to higher binding energy. (FOV = 4 μm, $h\nu = 200$ eV.)

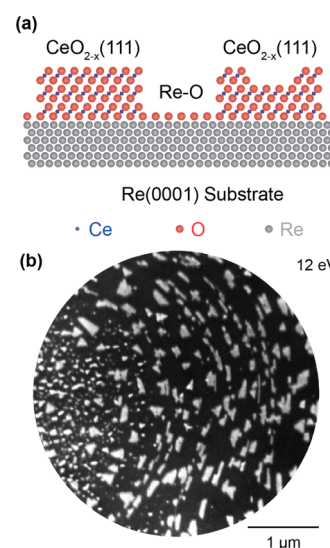


Figure 3. Structural model and LEEM of a 0.8 MLE CeO_{2-x}(111)/Re(0001) film. (a) Model of the ceria film, composed of islands 3 O–Ce–O trilayers thick with occasional steps down in the centers. (oxygen, red; rhenium, gray; cerium, blue) (b) Bright-field LEEM image showing the isolated ceria islands distributed across the Re(0001) substrate. (FOV = 4 μm, $E = 12$ eV.)

Re(0001) surface ($26 \pm 5\%$), which when combined with the magnitude of the initial cerium dose (0.8 ± 0.1) ML also yields a thickness estimate of $\sim 3 \pm 1$ trilayers. From earlier STM investigations of similar coverage CeO_{2-x}(111) films on Pt(111), an island thickness of ~ 3 trilayers is a common motif.^{4,19}

Oxygen 1s photoelectron spectroscopy was also carried out using the energy-filtered mode of the XPEEM instrument, the results of which are shown in Figure 4. The XPEEM image

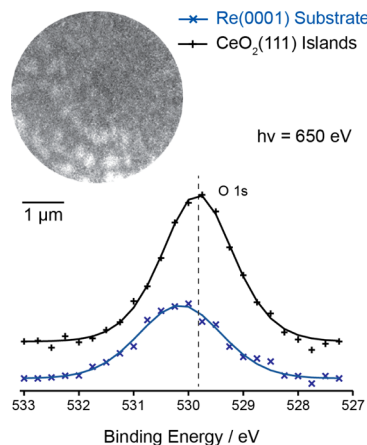


Figure 4. XPS from the Re(0001) substrate and the $\text{CeO}_{2-x}(111)$ islands as well as XPEEM of the O 1s region of a 0.8 MLE $\text{CeO}_{2-x}(111)$ ultrathin film on Re(0001). The inset energy-filtered XPEEM image (corresponding to a binding energy of 530 eV) displays some contrast between the ceria islands (bright regions) and the Re substrate with the greatest difference visible for the larger islands. The spectra are offset vertically for clarity. (FOV = 4 μm , $h\nu = 650$ eV.)

(FOV = 4 μm , same region as in Figure 2) obtained at a binding energy of 530 eV does not display very clear contrast between the ceria islands and the Re(0001) substrate due to the Re–O layer that extends across the substrate. A number of more intense areas are visible which coincide with the larger dark patches (wider ceria islands) observed in Figure 2, but the island edges are much more poorly defined. Regions of interest corresponding to the islands and the substrate were therefore identified by mapping from the Re 4f XPEEM image in Figure 2 to enable the extraction of spectra solely from the ceria

(black) and substrate (blue) from the O 1s XPEEM data, as displayed in Figure 4.

After fitting, it is observed that the Re(0001)-O O 1s peak is at 530.2 eV B.E. and the $\text{CeO}_{2-x}(111)$ O 1s is at 529.8 eV. The latter is in good agreement with the literature for a reduced $\text{CeO}_{2-x}(111)$ film.²³ The detection of the slightly shifted Re–O peak and the ability to attribute it to the substrate demonstrate the strength of spatially resolved XPS. The greater area-normalized intensity of the ceria O 1s is attributed to the larger amount of oxygen present in the islands relative to the substrate surface oxide. A shoulder peak at ~ 2 eV higher binding energy is common on ceria surfaces and is characteristic of hydroxyl species.²⁴ No such peak is observed on either the ceria or the substrate in this study, suggesting that the $\text{CeO}_{2-x}(111)$ is not hydroxylated under the measurement conditions.

In order to determine the oxidation state of the ceria films, resonant XPS of the valence band (VB) region was carried out using the energy-filtered XPEEM mode. The use of resonant photoelectron spectroscopy on ultrathin ceria films is well-established and provides very high sensitivity toward small changes in the oxidation state, especially in comparison with the traditional method of deconvolution of Ce 3d spectra.¹² Spectra are recorded using photon energies corresponding to off-resonance at 115 eV, on-resonance for Ce^{3+} ($4f^1$) at 120.5 eV, and on-resonance for Ce^{4+} ($4f^0$) at 123.5 eV.^{11,12} Figure 5 illustrates the procedure for extracting the VB spectra from the XPEEM images. In the energy-filtered mode, images (FOV = 4 μm) are acquired at 0.25 eV intervals across the VB region. By selecting regions of interest from these images it is then possible to extract spectra from regions extending over lengths of several tens nm. The spectra displayed in Figure 5 have been extracted from within the ceria islands (black curve) and Re(0001) substrate (blue curve) as identified by LEEM and the Re 4f XPEEM in Figure 2. They can be separated into three main regions according to their origin. (i) 8–12 eV binding energy; states are dominated by the Re(0001) oxide layer, the highest intensity in the corresponding XPEEM image (B.E. 9.25 eV) is therefore from the substrate so the ceria islands

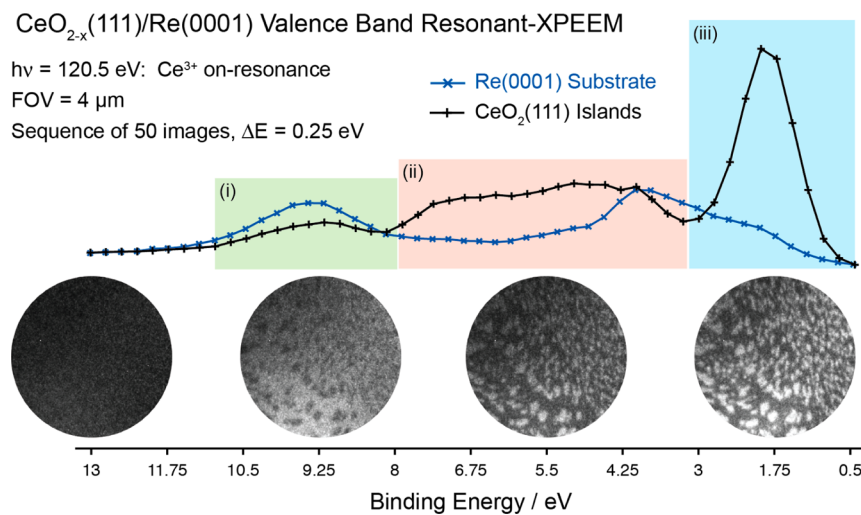


Figure 5. Energy-filtered XPEEM images and spectra of the valence band region of a 0.8 MLE $\text{CeO}_{2-x}(111)/\text{Re}(0001)$ film obtained on-resonance for the Ce 4d-4f excitation. The blue spectrum is obtained by sampling areas of the Re(0001) substrate between the ceria islands as identified in LEEM and Re 4f XPEEM (Figure 2) and the black spectrum is from the ceria islands. The VB region can be split into three main parts: (i) Re–O states dominate; the brightest contrast in the XPEEM images is on the Re(0001) substrate (ceria islands appear dark) and (ii and iii) Ce 4f and O 2p states are the dominant contribution, with (ii) corresponding to Ce^{4+} and (iii) to Ce^{3+} respectively.¹¹ The ceria islands appear bright in XPEEM images of regions (ii) and (iii). (FOV = 4 μm , $h\nu = 120.5$ eV.)

appear as dark patches. (ii)/(iii) 0–8 eV binding energy; states are dominated by O 2p and Ce 4f (ii, Ce⁴⁺; iii, Ce³⁺), where the ceria islands appear brightest in the associated XPEEM images. The clear contrast between the ceria islands and the substrate in the XPEEM images (B.E. of 5.5 and 1.75 eV) enables the application of drift-correction between images, improving the quality of the spectra by permitting high-confidence identification of regions of interest purely from within the islands.

VB spectra collected solely from the ceria islands are displayed in Figure 6 at three photon energies: on-resonance

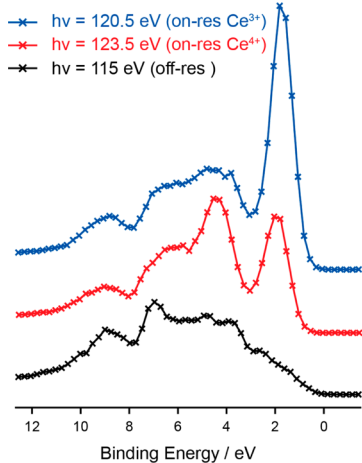


Figure 6. Valence band XPS spectra obtained from energy-filtered XPEEM images of a 0.8 MLE CeO_{2-x}(111)/Re(0001) film at photon energies of 120.5, 123.5, and 115 eV corresponding to on-resonance for Ce³⁺ (blue), Ce⁴⁺ (red), and off-resonance (black), respectively. Only areas within the ceria islands were sampled to ensure that any influence of the substrate is minimized. The spectra are offset vertically for clarity.

for Ce³⁺ ($h\nu = 120.5$ eV, blue curve), on-resonance for Ce⁴⁺ ($h\nu = 123.5$ eV, red curve), and off-resonance ($h\nu = 115$ eV, black curve). The resonant enhancements for the Ce³⁺ peak at 2 eV B.E. and Ce⁴⁺ peak at 4.25 eV B.E. are clear. Spectra have been normalized to the photon flux as measured on an Au mesh. VB spectra extracted from the substrate in between the ceria islands do not display any dependence on photon energy, confirming a lack of Ce in the regions between the ceria islands.

Subtracting the off-resonance spectrum from each of the on-resonance spectra yields the difference spectra displayed in Figure 7 where the intensities of the Ce³⁺ and Ce⁴⁺ resonant features are represented by DCe³⁺ and DCe⁴⁺. The ratio of these is termed the resonant enhancement ratio (RER = DCe³⁺/DCe⁴⁺) and is proportional to the Ce³⁺/Ce⁴⁺ ratio of the film.²⁵ Fitting the resonant features in Figure 7 yields a RER = 3 ± 0.3 for the islands in this study, which corresponds to an approximate overall stoichiometry of CeO_{1.63}.²⁶ This method probes only ~0.5 nm into the film²² and therefore is highly sensitive toward the presence of oxygen vacancies within the top couple of layers of the ceria. Such a heavily reduced film is consistent with the preparation method where the oxidation time was relatively short (10 min); STM images of similarly prepared films display high densities of surface oxygen vacancies.⁴

The XPEEM images which yielded the VB spectra in Figure 6 were subject to a large amount of thermal and instrumental drift, which limited the ultimate lateral resolution. To examine any lateral variations in oxidation state, another approach was

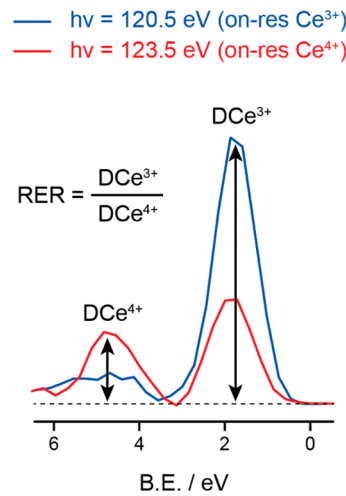


Figure 7. Difference spectra obtained from energy-filtered XPEEM of the valence band of a 0.8 MLE CeO_{2-x}(111)/Re(0001) film. The difference spectra were calculated by subtracting the off-resonance spectrum from the two on-resonance spectra (red and blue) in Figure 6; the resonant enhancement ratio (RER = DCe³⁺/DCe⁴⁺) is indicated.

used. The photon energy was fixed (120.5 eV, corresponding to Ce³⁺ on-resonance), and high resolution images were obtained on top of the Ce³⁺ (2 eV B.E.) and Ce⁴⁺ (4.25 eV B.E.) features as shown in Figure 8. The images are background corrected and then divided to give a measure of any variations in the Ce³⁺/Ce⁴⁺ ratio. From the image in Figure 8 it is observed that all of the islands have nearly the same intensity, and therefore this Ce³⁺/Ce⁴⁺ ratio is uniform across the film. A number of islands

VB XPEEM: Ce³⁺/Ce⁴⁺ ratio

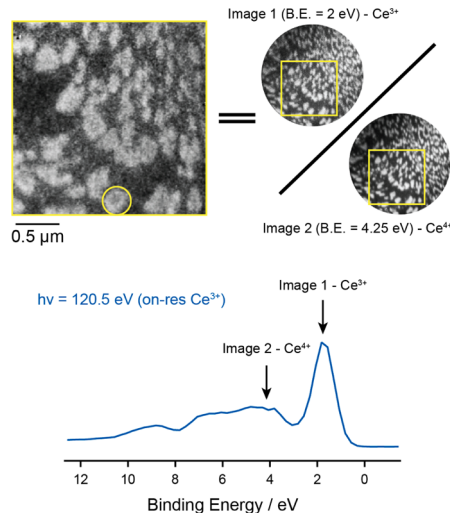


Figure 8. Energy-filtered XPEEM image and spectrum of the valence band region of a 0.8 MLE CeO_{1.63}(111)/Re(0001) film obtained at a photon energy of 120.5 eV which corresponds to on-resonance for the Ce³⁺ contribution to Ce 4f. The image displayed was obtained by dividing images obtained at binding energies of 2 and 4.25 eV and shows the ratio between the Ce³⁺ and Ce⁴⁺ components present in the ceria islands. It is observed that there is near-uniform stoichiometry across the film. The island highlighted with a yellow circle displays a region of reduced intensity in its center due to a height variation of the ceria.

do display a darker feature in the middle (one of which is highlighted), and this change in contrast is due to occasional height variations and holes in a few of the islands. Such holes, where one layer of the ceria is not fully formed, are commonly observed in the center of the islands on similar ultrathin films.¹¹ Some instances of this can be seen in the LEEM image in Figure 3b, and this is also illustrated in the model in Figure 3a.

CONCLUSIONS

Ultrathin $\text{CeO}_{2-x}(111)$ films have been prepared on $\text{Re}(0001)$ as a model catalyst system, and their structure investigated with LEEM and synchrotron-radiation based XPEEM. Rotational domains are observed in LEED and LEEM, and dark-field imaging permits identification of ceria islands up to a few hundred nanometres wide. Energy-filtered XPEEM of the $\text{Re}\ 4f$ levels indicates the presence of a $\text{Re}-\text{O}$ oxide layer extending across the entire surface, including underneath the ceria islands. Resonant XPEEM of the $\text{Ce}\ 4f$ contribution to the valence band allows the stoichiometry of the film to be determined as $\text{CeO}_{1.63}$, and high-resolution XPEEM imaging of the oxidation state indicates the near-uniformity of this stoichiometry between the different ceria islands that make up the film.

AUTHOR INFORMATION

Corresponding Author

*Tel: +44 (0)20 7679 7979. Fax: +44 (0)20 7679 0595. E-mail: g.thornton@ucl.ac.uk.

Notes

The authors declare no competing financial interest.

ACKNOWLEDGMENTS

The authors thank Dr. Chris Muryn for helpful discussions. This work was supported by the EU COST1104 and the European Research Council Advanced Grant ENERGYSURF (GT).

REFERENCES

- Trovarelli, A.; de Leitenburg, C.; Boaro, M.; Dolcetti, G. The Utilization of Ceria in Industrial Catalysis. *Catal. Today* **1999**, *50*, 353–367.
- Fu, Q.; Saltsburg, H.; Flytzani-Stephanopoulos, M. Active Nonmetallic Au and Pt Species on Ceria-Based Water-Gas Shift Catalysts. *Science* **2003**, *301*, 935–938.
- Rodriguez, J. A.; Ma, S.; Liu, P.; Hrbek, J.; Evans, J.; Perez, M. Activity of CeO_x and TiO_x Nanoparticles Grown on Au(111) in the Water-Gas Shift Reaction. *Science* **2007**, *318*, 1757–1759.
- Grinter, D. C.; Ithnin, R.; Pang, C. L.; Thornton, G. Defect Structure of Ultrathin Ceria Films on Pt(111): Atomic Views from Scanning Tunnelling Microscopy. *J. Phys. Chem. C* **2010**, *114*, 17036–17041.
- Kaemena, B.; Senanayake, S. D.; Meyer, A.; Sadowski, J. T.; Falta, J.; Flege, J. I. Growth and Morphology of Ceria on Ruthenium (0001). *J. Phys. Chem. C* **2013**, *117*, 221–232.
- Wilson, E. L.; Chen, Q.; Brown, W.; Thornton, G. CO Adsorption on the Model Catalyst Pd/CeO_{2-x}(111)/Rh(111). *J. Phys. Chem. C* **2007**, *111*, 14215–14222.
- Senanayake, S. D.; Sadowski, J. T.; Evans, J.; Kundu, S.; Agnoli, S.; Yang, F.; Stacchiola, D.; Flege, J. I.; Hrbek, J.; Rodriguez, J. A. Nanopattering in CeO_x/Cu(111): A New Type of Surface Reconstruction and Enhancement of Catalytic Activity. *J. Phys. Chem. Lett.* **2012**, *3*, 839–843.
- Grinter, D.; Thornton, G. In *Oxide Ultrathin Films: Science and Technology*; Pacchioni, G., Valeri, S., Eds.; Wiley-VCH: Weinheim, Germany, 2012.
- Agnoli, S.; Onur Menteş, T.; Niño, M. A.; Locatelli, A.; Granozzi, G. A LEEM/ μ -LEED Investigation of Phase Transformations in TiO_x/Pt(111) Ultrathin Films. *Phys. Chem. Chem. Phys.* **2009**, *11*, 3727–3732.
- Lovis, F.; Hesse, M.; Locatelli, A.; Menteş, T. O.; Niño, M. A.; Lilienkamp, G.; Borkenhagen, B.; Imbihl, R. Self-Organization of Ultrathin Vanadium Oxide Layers on a Rh(111) Surface during a Catalytic Reaction. Part II: A LEEM and Spectromicroscopy Study. *J. Phys. Chem. C* **2011**, *115*, 19149–19157.
- Matharu, J.; Cabailh, G.; Lindsay, R.; Pang, C. L.; Grinter, D. C.; Skála, T.; Thornton, G. Reduction of Thin-Film Ceria on Pt(111) by Supported Pd Nanoparticles Probed with Resonant Photoemission. *Surf. Sci.* **2011**, *605*, 1062–1066.
- Matolin, V.; Matolinová, I.; Sedláček, L.; Prince, K. C.; Skála, T. A Resonant Photoemission Applied to Cerium Oxide Based Nanocrystals. *Nanotechnology* **2009**, *20*, 215706.
- Schmidt, T.; Heun, S.; Slezak, J.; Diaz, J.; Prince, K. C.; Lilienkamp, G.; Bauer, E. SPELEEM: Combining LEEM and Spectroscopic Imaging. *Surf. Rev. Lett.* **1998**, *05*, 1287–1296.
- Locatelli, A.; Aballe, L.; Mentes, T. O.; Kiskinova, M.; Bauer, E. Photoemission Electron Microscopy with Chemical Sensitivity: SPELEEM Methods and Applications. *Surf. Interface Anal.* **2006**, *38*, 1554–1557.
- Gu, C.; Wu, X.; Olson, C.; Lynch, D. “ γ - α ” Phase Transition of Monolayer Ce on W(110). *Phys. Rev. Lett.* **1991**, *67*, 1622–1625.
- Grinter, D. C. Manuscript in preparation.
- Grinter, D. Surface Studies of Metal Oxide Catalysts and Ultrathin Films. *Ph.D. Thesis*; University College London: London, 2011; pp 1–227.
- Castellarin-Cudia, C.; Surnev, S.; Schneider, G.; Podlucky, R.; Ramsey, M.; Netzer, F. P. Strain-Induced Formation of Arrays of Catalytically Active Sites at the Metal-Oxide Interface. *Surf. Sci.* **2004**, *554*, L120–L126.
- Luches, P.; Pagliuca, F.; Valeri, S. Morphology, Stoichiometry, and Interface Structure of CeO₂ Ultrathin Films on Pt(111). *J. Phys. Chem. C* **2011**, *115*, 10718–10726.
- Wilson, E. L.; Grau-Crespo, R.; Pang, C. L.; Cabailh, G.; Chen, Q.; Purton, J. A.; Catlow, C. R. A.; Brown, W.; de Leeuw, N. H.; Thornton, G. Redox Behavior of the Model Catalyst Pd/CeO_{2-x}/Pt(111). *J. Phys. Chem. C* **2008**, *112*, 10918–10922.
- Tysoe, W. T.; Zaera, F.; Somorjai, G. An XPS Study of the Oxidation and Reduction of the Rhodium-Platinum System under Atmospheric Conditions. *Surf. Sci.* **1988**, *200*, 1–14.
- Tanuma, S.; Powell, C. J.; Penn, D. R. Calculations of Electron Inelastic Mean Free Paths (IMFPs). IV. Evaluation of Calculated IMFPs and of the Predictive IMFP Formula TPP-2 for Electron Energies between 50 and 2000 eV. *Surf. Interface Anal.* **1993**, *20*, 77–89.
- Lykhach, Y.; Johánek, V.; Aleksandrov, H. A.; Kozlov, S. M.; Happel, M.; Skala, T.; Petkov, P. S.; Tsud, N.; Vayssilov, G. N.; Prince, K. C.; Neyman, K. M.; Matolin, V.; Libuda, J. Water Chemistry on Model Ceria and Pt/Ceria Catalysts. *J. Phys. Chem. C* **2012**, *116*, 12103–12113.
- Zhao, X.; Ma, S.; Hrbek, J.; Rodriguez, J. A. Reaction of Water with Ce–Au(111) and CeO_x/Au(111) Surfaces: Photoemission and STM Studies. *Surf. Sci.* **2007**, *601*, 2445–2452.
- Staudt, T.; Lykhach, Y.; Tsud, N.; Skala, T.; Prince, K. C.; Matolin, V.; Libuda, J. Ceria Reoxidation by CO₂: A Model Study. *J. Catal.* **2010**, *275*, 181–185.
- Matolin, V.; Libra, J.; Škoda, M.; Tsud, N.; Prince, K. C.; Skála, T. Methanol Adsorption on a CeO₂(111)/Cu(111) Thin Film Model Catalyst. *Surf. Sci.* **2009**, *603*, 1087–1092.